A Novel Compact Planar Spiral-shaped Antenna

Bing Xiao, Lei Zhong, Jing-Song Hong, and Song-Lin Li

The Institute of Applied Physics
University of Electronic Science and Technology of China, Chengdu, 610054
bxuestc@gmail.com

Abstract **─** A novel compact spiral antenna with planar feed structure is presented. The proposed antenna is a two-arm Archimedean spiral antenna, which has similar properties of wideband and circular polarization to traditional one. A remarkable improvement of the proposed antenna is the completely planar feed structure. The whole antenna is compact， its spiral diameter is only 23.2mm and the balun is also small. It has an impedance bandwidth of 67% from 4.5GHz to 9GHz and a 4-dB axial-ratio bandwidth of 46.67% ranging from 4.6 GHz to 7.4 GHz. It can be widely used in wideband planar antenna array and other low profile applications.

Index Terms **─** circular polarization, planar antenna arrays, spiral antennas, wideband antennas.

I. INTRODUCTION

Wideband planar antennas have been widely used in aircraft, satellite, radar, remote control, telemetry, etc., especially when bandwidth, profile, conformal installation, weight and cost are main concerns of the users. In terms of polarization of wideband planar antenna, circular polarization (CP) is more attractive than linear polarization. CP can facilitate easy orientations between transmitters and receivers and has high degree of mobility, weather penetration, and reduction in multipath reflections and other kinds of interferences [1].

Several kinds of wideband antennas can accommodate the demand of both planar structure and circular polarization. Microstrip antenna is the most commonly used antenna. Basically, there are two techniques to generate circular polarization for a single microstrip patch. One is to excite the square or circular patch by two orthogonally located feeds. The other is to employ an irregular physically perturbed patch that is excited by a single feed. However, two feed points greatly complicate the feed network, while irregular shape of the patch breaks up the symmetry radiation [2, 3]. Most of all, microstrip antenna is an inherent narrow band antenna, so it is difficult to expand bandwidth significantly. Therefore, new techniques of planar wideband circularly polarized antenna should be explored.

Spiral antennas have emerged as leading candidates for various commercial and military applications requiring wideband circularly polarized operation [4]. Spiral antennas are inherent frequency-independent antennas. For instance, they can achieve bandwidth up to 40:1 [5] and offer high-quality circular polarization, because their input impedances are near constant over the entire operating frequency range. In recent years, various spiral antennas have been developed [6-9].

However, conventional spiral antenna is always fed by a balun, which is perpendicular to the spiral plane in the center [10-12]. Therefore, they cannot be completely planar and encounter serious difficulties in the planar integration of spiral antenna.

To design a planar feed structure for spiral antenna, several attempts have been made over the past few years [13-16]. Some authors use slotlines instead of strips for the convenience of planar feed [13-15]. As we all know, slotline is a dispersion transmission line, whose phase velocity varies with the frequency. Thus it will affect the group delay time of wideband antenna. Some other spiral antennas are designed by strips, but they do not have a compact and simple structure for microstrip feed [16]. Apparently, a compact planar spiral

Submitted On: Mar. 28, 2012
Accepted On: Dec. 16, 2012

antenna fed by microstrip is much more adaptable to low profile applications, such as planar antenna array.

This article investigates the possibility of a completely planar spiral antenna. The antenna is a spiraled coplanar stripline (CPS) fed by a novel compact microstrip-to-CPS balun. It shows wideband left hand circular polarization (LHCP) on front side and right hand circular polarization (RHCP) radiation pattern on back side. The simulation and experimental results show an impedance bandwidth of 67% from 4.5GHz to 9GHz and 4-dB axial-ratio bandwidth of 46.67% from 4.6 GHz to 7.4 GHz, whose radiation characteristics are similar to center-fed spiral antenna.

II. DESIGN OF SPIRALS

Figure 1 shows the configuration of the spirals. A CPS line is wound around the center. Thus, the two strips of CPS become an inner spiral and an outer spiral. The distance from the center to a strip is defined as r, which is expressed as $r=r_0+a\varphi$, where r_0 is the initial radius, a is the growing rate, and φ is the winding angle. This expression comes from the classical Archimedean spiral antenna [11].

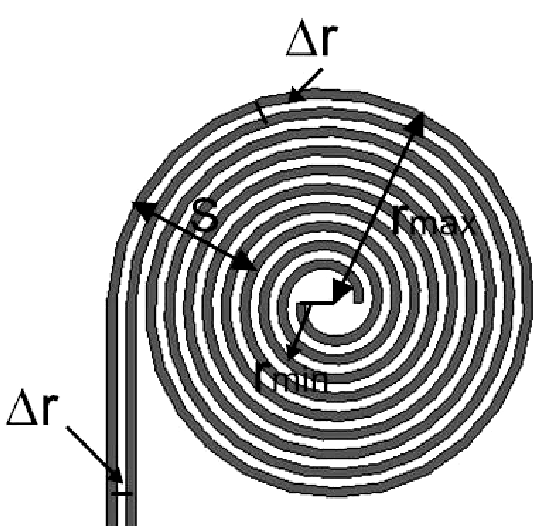

Fig. 1. Configuration of the spirals.

In order to get a symmetrical structure, the end of outer spiral is wound half a turn further in the center. According to the band theory [11], the lower frequency limit of the operation band can be determined by judging whether the currents in neighboring arms are in phase. The start of two spiral strips is a typical CPS, and the currents on the two strips are in antiphase. Therefore, the electromagnetic field is bound between the two strips and does not radiate.

However, the different radii lead to a different length between the two strips of CPS while winding. If the different length is equal to half a wavelength, the currents will be in phase, and the electromagnetic field will radiate. When a CPS line (two spiral strips) is wound by 360°, the phase difference is $2\pi\Delta r$ (Δr is the distance between every two adjacent spiral strips). Thus, we assume the radiation occurs at a distance $s \sim s+\Delta r$ along the circumference and CPS is wound by n turns, then

$$n \cdot 2\pi \cdot \Delta r = \frac{\lambda_g}{2} . \quad (1)$$

So

$$s = 2n \cdot \Delta r = \frac{\lambda_g}{2\pi} , \quad (2)$$

where λg is the guided wavelength on the spiral arms. It is worthwhile to note that the distance s is independent from both the arm spacing Δr and the number of turn n. It is only proportional to the guided wavelength of corresponding frequency. Apparently, s cannot exceed the radius of radiation part r_{max}. If the minimum frequency of the antenna is f_{min}, the maximal s can be calculated by

$$s_{(f\min)} = \frac{c_0}{2\pi\sqrt{\varepsilon_{eff}} \cdot f_{\min}} , \quad (3)$$

where c_0 is the speed of light in free space and ε_{eff} is the effective relative dielectric constant of CPS. As we use a 0.8-mm-thick RO4003C substrate (relative dielectric constant ε_r=3.38), the effective relative dielectric constant is 2.04 [17]. Thus $s_{(fmin)}$ is calculated as 5.8mm, according to (3).

In fact, r_{max} should be twice as long as $s_{(fmin)}$ in reality. Based on the principles mentioned above, if $r_{max} = s_{(fmin)}$, the effective radiation area of the minimum frequency should be the center point of the spiral strips. Since the currents are cut at this point, there cannot be any effective radiation here. So we define the initial value of r_{max} as 11.6mm. And r_{min} is designed as 1.8mm in order to keep the end of two spirals apart in the center.

Additionally, strip width Ws and gap width Wg (Wg=Δr-Ws) are designed as equal value. In the classical theory of Archimedean spiral antenna, a self-complementary structure is modeled, when strip width is equal to gap width. The largest bandwidth and the lowest input impedance can be achieved at the same time. As spiral antenna is a travelling wave structure, the signal travels along spirals and the intensity decays gradually. Hence the input impedance of the antenna is the same as the characteristic impedance of CPS feed line.

In order to match the spirals to a 50Ω microstrip line, $Ws=Wg$=0.6mm are set as initial value for lower input impedance.

Growing rate of spirals, determined by Wg, Ws, and r_{max}, is set as 0.38mm/rad.

Figure 2 shows the simulated electric field intensity distribution at four different frequency points (4.7 GHz, 5.6 GHz, 6.5 GHz and 7.4 GHz). The bright area represents high intensity while the dark area represents low intensity. Radiation occurs where high intensity decreases to low intensity, because the reduced intensity has become radiation energy and radiated outward. Consistent with the theoretical analysis, the higher the frequency is, the outer the radiation area locates.

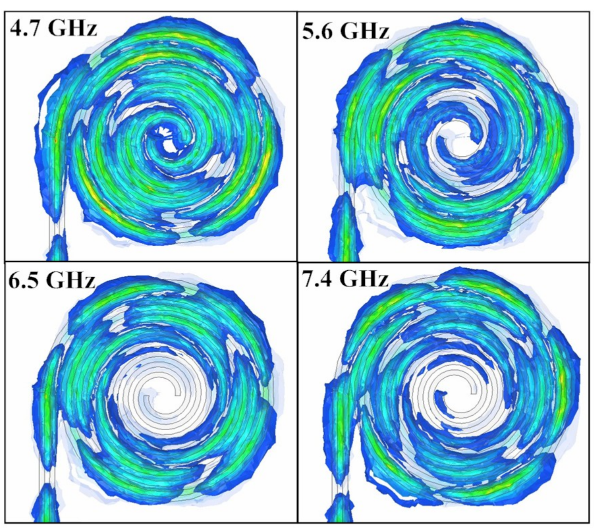

Fig. 2. Electric field intensity distributions at four different frequencies.

III. DESIGN OF CPS-TO-MICROSTRIP BALUN

The input impedance of spirals is decided by both strip width Ws and gap width Wg. Figure 3 shows the simulated real and imaginary parts of the input impedance of the spirals. Below 5GHz the input impedance changes dramatically with frequency and the spirals are difficult to match with a balun. Ranging from 5GHz to 9GHz, the two curves are less oscillatory, and the magnitude of the input impedance is nearly a constant with an average of 175Ω. We can design a microstrip-to-CPS balun to feed the CPS structure in this band, where both field matching and impedance matching need to be considered [18].

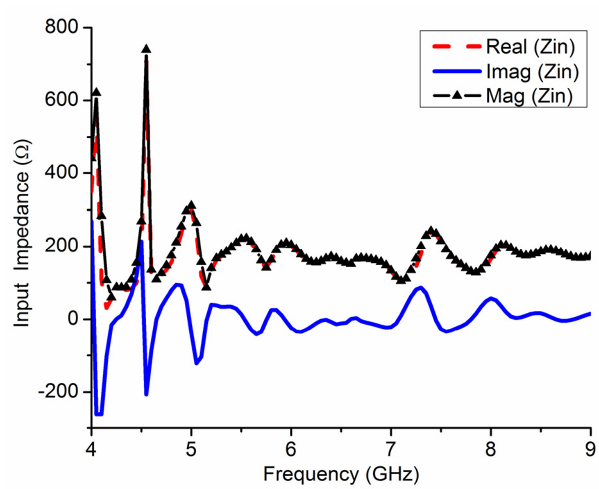

Fig. 3. Real part, imaginary part and magnitude of the input impedance of the spirals.

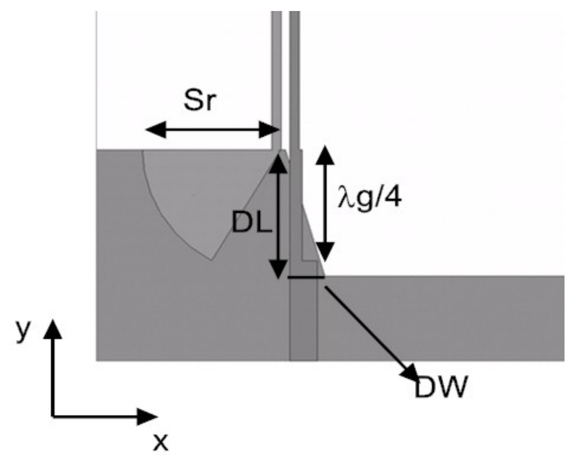

Fig. 4. Wide-band CPS-to-microstrip balun.

Recently, several CPS-to-microstrip baluns on low dielectric-constant substrate have been reported [19-21]. These baluns use a long smooth tapered microstrip line to match high characteristic impedance of CPS. The proposed structure in this paper is compact and satisfying.

Figure 4 shows the proposed wide-band CPS-to-microstrip balun based on coupling method.

The transition consists of a microstrip stepped matching transformer, a radial stub and a quadrangle-defected ground.

Since the input impedance of the CPS is about 175Ω, a 94Ω quarter-wavelength transformer is assigned to match 175Ω and 50Ω.

As the electric field in the microstrip line is parallel to z-axis and the electric field in the CPS is parallel to x-axis, a 90°electric-field rotation is needed. So a quadrangle defected ground structure (DGS) is employed to rotate the direction of electric field. The DGS can avoid mutual interference by keeping spirals and ground apart. This balun has advantages of wide bandwidth, low loss, and compactness.

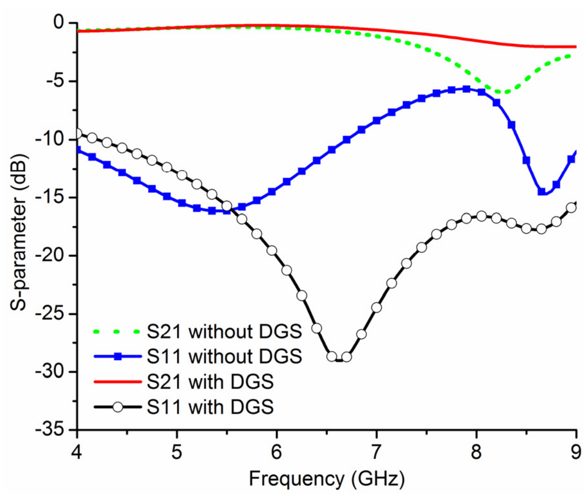

Fig. 5. S21 and S11 curves of the balun with and without the quadrangle DGS.

Figure 5 shows S21 and S11 curves of the balun with and without the quadrangle DGS. As shown in Fig. 5, the transmission coefficient is higher and the return loss is lower when the ground is truncated.

Since the quarter-wave radial stub can be seen as virtual short, it is in equal potential with the ground plane. Thus at the start of radial stub, electric field on CPS begins to couple into the ground. When the ground plane is gradually formed, the electric field intensity between strip and ground is gradually stronger (microstrip) and that between two strips (CPS) is gradually weaker. So we can reduce the reflection loss to the maximum extent, and the quasi-TEM mode of microstrip is obtained.

Additionally, *Sr* should theoretically be quarter guided wavelength of the center frequency. However, according to the results of full wave simulation, *Sr* has a relatively big impact on the axial ratio of the spiral antenna, which is probably because *Sr* decides the phase difference at the start of CPS. *Sr* is defined as 6.1mm to balance the transmission efficiency and axial ratio.

IV. SIMULATION AND MEASUREMENT RESULTS

Based on the analysis above and simulations results with Ansoft HFSS 13, the detailed dimensions of the proposed antenna are showed in Table 1.

The validity of the presented design was tested by a prototype, as shown in Fig. 6. The manufactured spiral antenna was tested by a vector network analyzer.

Figure 7 shows the simulated and measured return loss of the proposed antenna. The bandwidth of 10 dB return loss covers from 4.5 to 9GHz.The LHCP and RHCP radiation patterns at 4.7 GHz, 5.6 GHz, 6.5 GHz and 7.4 GHz are shown in Fig. 8 (a)-(d) respectively. The radiation patterns are similar to conventional center-fed spiral antenna at 4.7 GHz, 5.6 GHz and 6.5 GHz, whereas at 7.4 GHz, the radiation pattern is degraded. This is because the asymmetry brought by the feed line has a greater impact when radiation occurs at outer part of spirals. Additionally the circular polarization property is also worse, as is shown in Fig. 9. If the radius of the spiral r_{max} increases, the radiation pattern and the axial ratio at higher frequency will be probably improved, but the size will be even bigger.

Table 1: Dimensions of the Proposed Antenna

Substrate: RO4003C (ε_r=3.38, tanδ=0.002, h=0.8mm)			
r_{max}	11.6 mm	***Ws***	0.6 mm
r_{min}	1.8 mm	***Wg***	0.6 mm
DL	9 mm	***Sr***	6.1 mm
DW	2.6 mm	$\lambda_g/4$	7.9 mm
a	0.38 mm/rad	***n***	4.5

Figure 9 shows the simulated broadside axial ratio versus frequency. Generally, the 4-dB axial ratio bandwidth covers from 4.6 GHz to 7.4 GHz. The simulated broadside gain is shown in Fig. 10.

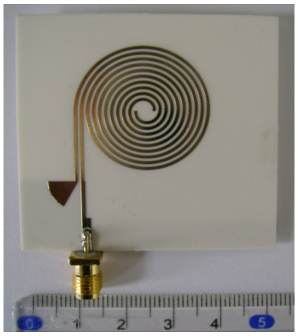
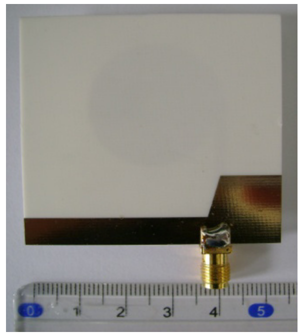

(a) The top view, (b) The bottom view,

Fig. 6. Photograph of the proposed antenna: (a) the top view, (b) the bottom view.

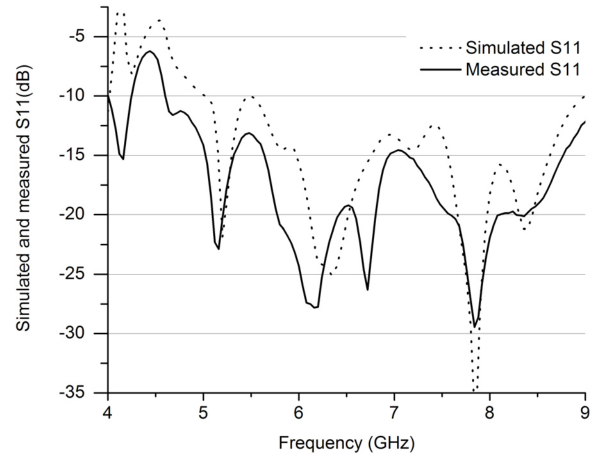

Fig. 7. The simulated and measured return loss.

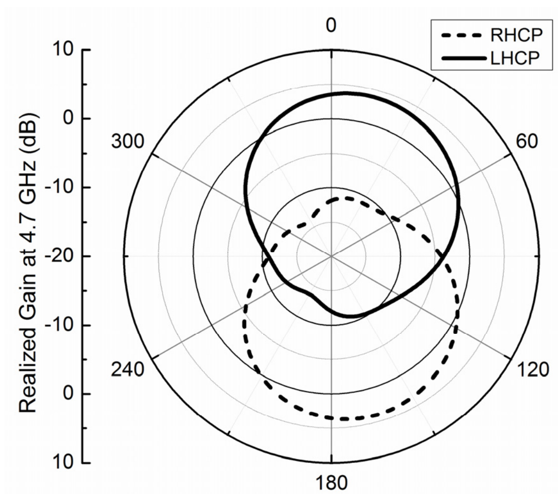

(a) 4.7 GHz,

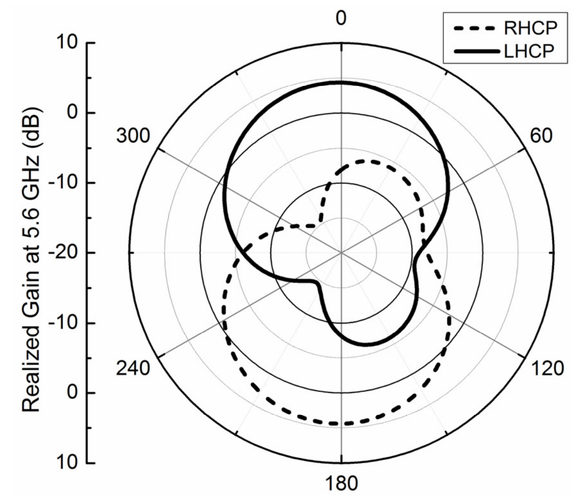

(b) 5.6 GHz,

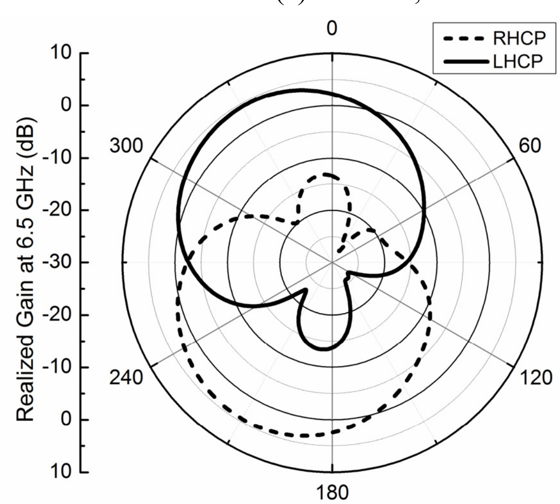

(c) 6.5 GHz,

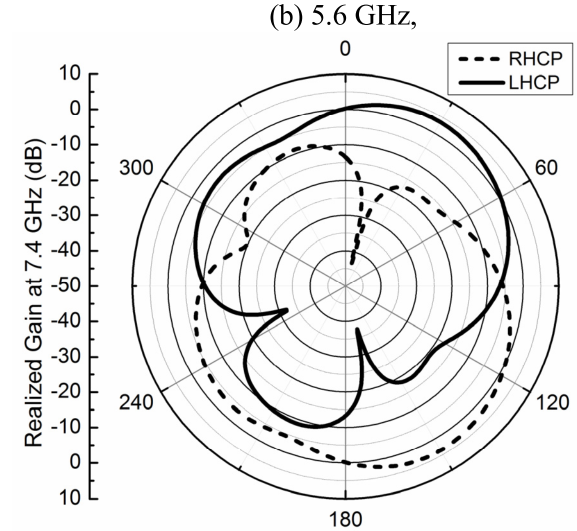

(d) 7.4 GHz,

Fig. 8. Radiation patterns at different frequencies, (a) 4.7 GHz, (b) 5.6 GHz, (c) 6.5 GHz and (d) 7.4 GHz.

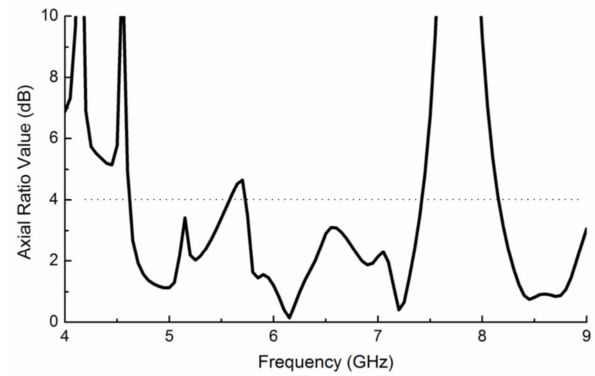

Fig. 9. Broadside axial ratio versus frequency.

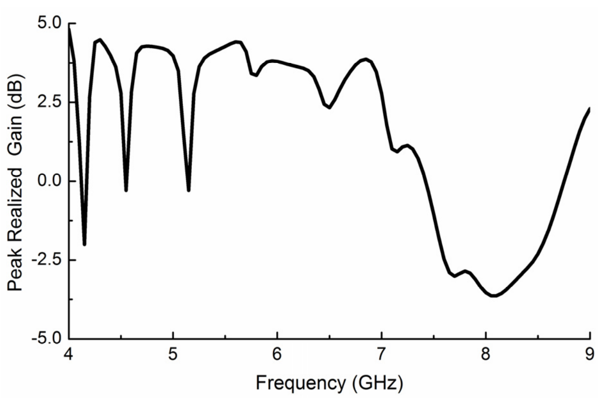

Fig. 10. Broadside gain versus frequency.

V. CONCLUSION

A compact planar spiral-shaped circularly polarized antenna is proposed. This antenna has a compact structure and wideband property, so it can be integrated in planar antenna arrays. However, the performance of this spiral antenna is not as excellent as the traditional center-fed one. Because the external feed destroys symmetry of spirals, and the ground of microstrip affects radiation characteristics especially at the higher frequency band. There is still much room for improvement of bandwidth and circular polarization for future research.

ACKNOWLEDGMENT

This work was supported by the National Natural Science Foundation of China (No.61172115 and No.60872029), the High-Tech Research and Development Program of China (No. 2008AA01Z206), the Aeronautics Foundation of China (No.20100180003), and the Fundamental Research Funds for the Central Universities (No.ZYGX2009J037).

REFERENCES

[1] R. Garg, *Microstrip Antenna Design Handbook*, Artech house publishers, 2001.

[2] A. Chen, Y. Zhang, Z. Chen, et al. "Development a Ka-Band Wideband Circularly Polarized 64-element Microstrip Antenna Array with Double Application of the Sequential Rotation Feeding Technique," *IEEE Antennas and Wireless Propagation Letters,* vol. 10, pp. 1270-1273, 2011.

[3] C. S. Ong, M. F. Karim, L. C. Ong, et al. "A Compact 2× 2 Circularly Polarized Antenna Array for Energy Harvesting," *Asia-Pacific Microwave Conference Proceedings (APMC)*, pp. 1977-1980, 2010.

[4] J. Dyson, "The Equiangular Spiral Antenna," *IRE Transactions on Antennas and Propagation.* vol. 7, no. 2, pp. 181-187, 1959.

[5] W. L. Stutzman, G. A. Thiele, *Antenna Theory and Design*, J. Wiley, 1998.

[6] N. Rahman, A. Sharma, M. Asfar, S. Palreddy, R. Cheung, "Dielectric Characterization and Optimization of Wide-band, Cavity-Backed Spiral Antennas," *Applied Computational Electromagnetics Society (ACES) Journal*, vol. 26, no. 2, pp. 123 - 130, February 2011.

[7] S. Palreddy, A. I. Zaghoul, R. Cheung, "Study of the Effects of the Back Cavityon a Broadband Sinuous Antenna and an Optimized Loaded Back Cavity," *Applied Computational Electromagnetics Society (ACES) Journal*, vol. 26, no. 8, pp. 660-666, August 2011.

[8] S. K. Khamas, G. G. Cook, "Optimised Design of a Printed Elliptical Spiral Antenna with a Dielectric Superstrate," *Applied Computational Electromagnetics Society (ACES) Journal*, vol. 23, no. 4, pp. 345-351, December 2008.

[9] C. Fumeaux, D. Baumann, R. Vahldieck, "FVTD Characterization of Substrate Effects for Archimedean Spiral Antennas in Planar and Conformal Configurations," *Applied Computational Electromagnetics Society (ACES) Journal,* vol. 20, no. 3, pp. 186-187, November 2005.

[10] E. Gschwendtner, W. Wiesbeck, "Frequency-Independent Antenna Concepts for the Use in Vehicles," *International Crimean Microwave and Telecommunication Technology*, pp. 39-42, 2000.

[11] J. Kaiser, "The Archimedean Two-Wire Spiral Antenna," *IRE Transactions on Antennas and Propagation ,* vol. 8, no. 3, pp. 312-323, 1960.

[12] M. Veysi, M. Kamyab, Bandwidth "Enhancement of Low-profile PEC-Backed Equiangular Spiral Antennas Incorporating Metallic Posts," *IEEE Trans. Antennas and Propagation,* vol. 99, no. 1, 2011.

[13] D. S. Filipovic, A. U. Bhobe, T. P. Cencich, “Low-Profile Broadband Dual-Mode Four-Arm Slot Spiral Antenna with Dual Dyson Balun Feed,” *IEE Proceedings Microwaves Antennas and Propagation*, pp. 527-533, 2005.
[14] W. Z. Wu, T. H. Chang, J. F. Kiang, “Broadband Slot Spiral Antenna with External Feed and Microstrip-to-Slotline Transition,” *IEEE APSI symp.*, pp. 767-770, 2004.
[15] E. Gschwendtner, D. Loffler, W. Wiesbeck, “Spiral Antenna with External Feeding for Planar Applications,” *IEEE Africon,* pp. 1011-1014, 1999.
[16] E. Gschwendtner, J. Parlebas, W. Wiesbeck, “Spiral Antenna with Planar External Feeding,” *29th European Microwave conference*, vol. 1, pp. 135-138, 1999.
[17] I. J. Bahl, P. Bhartia, *Microwave Solid State Circuit Design*, Wiley-Interscience, 2003.
[18] J. S. Izadian, S. M. Izadian, *Microwave Transition Design*, Artech House, 1988.
[19] Y. H. Suh, K. Chang “A Wideband Coplanar Stripline to Microstrip Transition,” *IEEE Microwave and Wireless Components Letters,* vol. 11, no. 1, pp. 28-29, 2001.
[20] T. Chiu, Y. S. Shen “A Broadband Transition Between Microstrip and Coplanar Stripline,” *IEEE Microwave and Wireless Components Letters,* vol. 13, no. 2, pp. 66-68, 2003.
[21] W. H. Tu, K. Chang, “Wide-Band Microstrip-to-Coplanar Stripline/Slotline Transitions,” *IEEE Trans. on Microwave Theory and Techniques,* vol. 54, no. 3, pp. 1084-1089, 2006.

Bing Xiao is a graduate student major in Radio Physics in the University of Electronic Science and Technology of China now. His research interests include antenna technology and wireless communication technique.

Lei Zhong is a graduate student major in Radio Physics in the University of Electronic Science and Technology of China now. His research interests include wideband antenna technology and wireless communication technique.

Jing-song Hong received the B.Sc. degree in electromagnetics from Lanzhou University, China, in 1991, and the M.Sc. and Ph. D. degrees in electrical engineering from the University of Electronic Science and Technology of China (UESTC), in 2000 and 2005, respectively. He is now a professor with UESTC. From 1991 to 1993, he was a Circuit Designer with the Jingjiang Radar Factory, Chengdu, China. From 1993 to 1997, he was a Testing Engineer with SAE Magnetics (HK) Ltd, Guangdong, China. From 1999 to 2002, he was a Research Assistant with the City University of Hong Kong. His research interest includes the use of numerical techniques in electromagnetics and the use of microwave methods for materials characterization and processing.

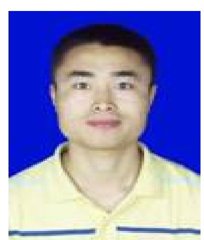

Song-lin Li is a graduate student major in Radio Physics in the University of Electronic Science and Technology of China now. His research interests include antenna technology and wireless charging technique.